



This is a repository copy of *Foam evolution inspired modeling for staged construction of ultra-dense small cell networks*.

White Rose Research Online URL for this paper:  
<http://eprints.whiterose.ac.uk/172202/>

Version: Published Version

---

**Article:**

Huang, Y., Hu, H., Zhang, J. [orcid.org/0000-0003-3750-6841](https://orcid.org/0000-0003-3750-6841) et al. (1 more author) (2021) Foam evolution inspired modeling for staged construction of ultra-dense small cell networks. IEEE Access. ISSN 2169-3536

<https://doi.org/10.1109/access.2021.3062207>

---

**Reuse**

This article is distributed under the terms of the Creative Commons Attribution (CC BY) licence. This licence allows you to distribute, remix, tweak, and build upon the work, even commercially, as long as you credit the authors for the original work. More information and the full terms of the licence here:  
<https://creativecommons.org/licenses/>

**Takedown**

If you consider content in White Rose Research Online to be in breach of UK law, please notify us by emailing [eprints@whiterose.ac.uk](mailto:eprints@whiterose.ac.uk) including the URL of the record and the reason for the withdrawal request.



[eprints@whiterose.ac.uk](mailto:eprints@whiterose.ac.uk)  
<https://eprints.whiterose.ac.uk/>

Received February 8, 2021, accepted February 15, 2021, date of publication February 24, 2021, date of current version March 5, 2021.

Digital Object Identifier 10.1109/ACCESS.2021.3062207

# Foam Evolution Inspired Modeling for Staged Construction of Ultra-Dense Small Cell Networks

YIXIN HUANG<sup>1</sup>, HAONAN HU<sup>2</sup>, (Member, IEEE),  
JILIANG ZHANG<sup>1</sup>, (Senior Member, IEEE),  
AND JIE ZHANG<sup>1,3</sup>, (Senior Member, IEEE)

<sup>1</sup>Department of Electronic and Electrical Engineering, The University of Sheffield, Sheffield S1 4ET, U.K.

<sup>2</sup>School of Communication and Information Engineering, Chongqing University of Posts and Telecommunications, Chongqing 400065, China

<sup>3</sup>Ranplan Wireless Network Design Ltd., Cambridge CB23 3UY, U.K.

Corresponding author: Jiliang Zhang (jiliang.zhang@sheffield.ac.uk)

This research was partially funded by the H2020 WAVECOMBE project.

**ABSTRACT** Small cells (SCs) are expected to be ultra-densely deployed in or close to the traffic hot-spots in the fifth generation (5G) mobile networks to provide wireless capacity cost-effectively. Traffic hot-spots change over time, which means SCs cannot be deployed in a one-off manner as macrocells normally do, rather they should be constructed in a staged process. Hence, mathematical models that capture the time-varying staged-construction process, are urgently needed for operators to effectively predict the construction period, but are currently lacking. In this paper, inspired by the foam bursting process—a natural phenomenon that can be observed in daily life such as hand-washing, we first propose a novel model that can predict the time-varying expectation and logarithmic variance of SC coverage areas. Then, we verify the model by real network deployment cases. Additionally, in order to extract parameters from historical base station deployment data, a parameter estimation algorithm is designed and verified. The findings of the paper reveal that mobile operators should construct ultra-dense SC networks in a staged manner like how larger foams split into smaller ones.

**INDEX TERMS** Dynamic modeling, staged construction, ultra-dense small cell network.

## I. INTRODUCTION

Heterogeneous network (HetNet) is a key enabling technology for the fourth generation (4G) and the fifth generation (5G) mobile networks. In a HetNet, macrocells are used to provide coverage and mobility support, while the ultra-densely deployed small cells (SCs) are used to provide a vast amount of capacity in the coverage area [1], [2]. With the advent of the 5G network, the explosive growth of traffic demand has turned network densification into a necessary condition for ensuring future network capacity [3]. Therefore, the densely deployed SC network is an effective approach for improving the network capacity and service probability.

Operators usually adopt a one-off layout strategy to build traditional third-generation (3G) and fourth-generation (4G) networks [4], [5]. This one-off deployment strategy is valid

for a cellular network with low-density base stations (BSs) because of its low design complexity, short construction time, and small labor cost. However, SC BSs will be ultra-densely deployed in the coming fifth-generation (5G) networks [2], [3], [6]–[9]. Traffic hot spots change with time due to the new business commercial, residential areas, etc. Consequently, the one-off deployed SC network may not meet the time-varying network capacity requirements [10]. In contrast, if operators divide the ultra-dense SC network construction into stages, the new SCs deployments can better meet emerging hot spots' network requirements. Moreover, the one-off deployment strategy will bring a huge one-time equipment cost and insertion cost, which requires a huge one-time investment [11]. This huge one-time investment challenge will bring additional risks of cash flow problems: the return on investment is low, and the cost may outweigh the money coming in [12]. Whereas, when an ultra-dense SC network is staged constructed, operators can open the

The associate editor coordinating the review of this manuscript and approving it for publication was Bong Jun David Choi<sup>1</sup>.

network to the public after completing the initial construction stage. Therefore, the operating revenue obtained from the earlier incomplete-network opening can cover parts of the network capital expenditures (CAPEX) and the operating expenditures (OPEX) [11] of the subsequent construction stages.

We define this new construction pattern as a staged construction (SCON) process, in which the expectation and variance of the BS coverage area change as the construction progresses with stages. This temporal change of BS coverage area distribution is closely related to the network performance. Therefore, mathematically modeling the variation of the time-varying BS coverage area distribution is crucial for operators to effectively predict the construction period required for network construction using the SCON approach. Specifically, this mathematical model can help operators formulate the corresponding SCON plan to finally achieve the target network performance.

Existing studies on dynamic networks have been proposed in the field of self-organizing networks and BS on/off switch handling [13]–[15]. In these researches, to improve the ultra-dense small cell network's energy efficiency, researchers have proposed different mathematical models that can automatically switch the state of SCs to respond to the fluctuating network traffic. These mathematical models can improve the network performance, such as network energy efficiency or the cell-edge throughput for the fully constructed networks. However, existing models ignore the dynamic network changes in the construction process [13]. To the best of our knowledge, the mathematical model to describe the under-constructed network, i.e., a network with time-varying BS distribution, has never been investigated before.

Interdisciplinary research often plays an essential role in accelerating disciplinary discovery in blank study fields such as physics-based or biology-based engineering [16]. As the first SCON network modeling, in the absence of existing research on the BS construction process mechanism, we introduce the process with similar evolution from physics-based engineering, i.e., the inverse foam bursting process, as a reference for the BS construction process [17]. The inverse process of bubble change during the foam bursting process is highly similar to the SC coverage change in SCON. During the foam bursting process, the bubble evolves from initial small average size and uniform distribution to eventual large average size and non-uniform distribution. By contrast, during the SCON process, the coverage area of SCs evolves from initial large average value and non-uniform distribution to eventual small average value and uniform distribution.

Therefore, to fill the gap in the dynamic modeling of ultra-dense small cell deployment using the SCON approach, we propose a novel time-varying mathematical model of BS distribution inspired by the foam distribution model to lay a foundation for this research field. Moreover, we provide a case study for operators to effectively make a trade-off

between the construction period and the service probability with the proposed model while designing a new SCON network.

The specific contributions of this work are summarized as follows:

- The expectation and the logarithmic variance of BS coverage areas, which are modeled as variables of the time-varying coverage area distribution in a point process, are employed as metrics of temporal network performance.
- The inverse foam bursting process is applied to the BS SCON model. The spatial-temporal mathematical expressions of the average and the logarithmic variance of BS coverage areas are derived.
- A Kolmogorov-Smirnov statistic [18] based estimation algorithm is proposed to extract parameters of the proposed model from actual Long-Term Evolution (LTE) BS spatial-temporal distributions.
- A method for computing the service probability of a new under-construction network using the proposed model is presented.

The rest of this paper is summarized as follows. Section II presents the framework of the time-varying ultra-dense SC network. Section III presents the modeling of the SCON network. Section IV presents the algorithms that can extract parameters from historical network construction data. Section V illustrates the validation based on the historical data and a case study for how operators weigh the construction period against the service probability with the proposed SCON model. Section VI concludes this paper.

## II. TIME-VARYING ULTRA-DENSE SMALL-CELL NETWORKS

Existing mathematical models usually assume that the BSs' locations follow a Poisson point process (PPP) [19], [20]. Calculations of network performance given from these models are tractable. The area distribution of Voronoi cells in PPP was simulated mathematically in [21]. Moreover, a network performance framework was provided for this mathematical modeling [22]. Let  $V$  be the area of a generic PPP-Voronoi cell, then:

$$f(V) \approx \frac{(\lambda c)^c V^{c-1} e^{-c\lambda V}}{\Gamma(c)}, \quad (1)$$

where  $\lambda$  is the density of BSs, and  $c$  is the fitting constant. When  $c$  is 3.5, this distribution fits the 2D PPP. According to (1), the expectation ( $V_{\text{extave}} \triangleq E[V]$ ), variance ( $S_V^2 \triangleq D[V] \triangleq E[(V - E[V])^2]$ ) and logarithmic variance ( $\sigma \triangleq D[\ln V]$ ) of  $V$  in PPP can be derived as:

$$V_{\text{ave}} = \frac{1}{\lambda}, \quad S_V^2 = \frac{1}{\lambda^2 c}, \quad \sigma = \ln \left( 1 + \frac{1}{c} \right). \quad (2)$$

Equations (2) show a bijection between the expectation and variance of the BS coverage areas when BSs' locations follow PPP. However, positions of SC BSs are affected by complex factors such as the change of hot-spots and the

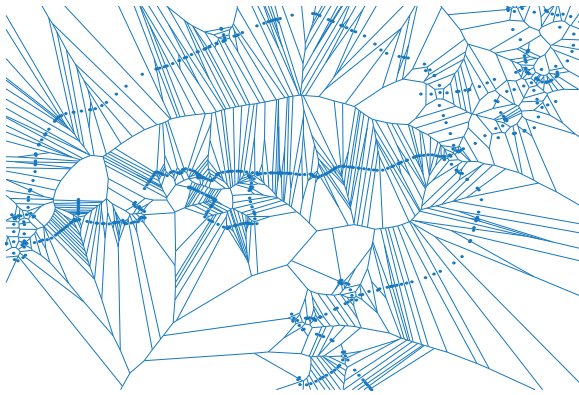


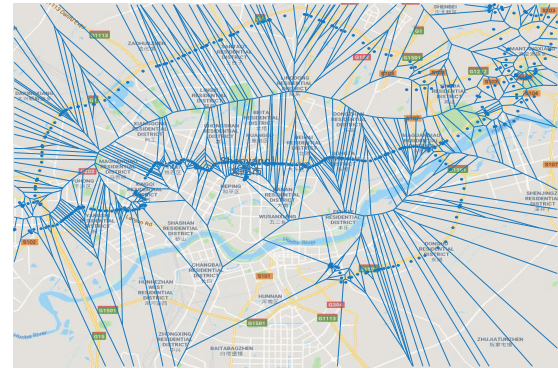
**FIGURE 1.** The Thiessen polygon area of each BS (on 31st, November, 2016) generated by Voronoi Tessellation.

constraints of the construction environments. Thus, the new hot spots are not uniformly distributed, which destroys the correlation between the expectation and variance of the BS coverage area. Therefore, closer to the actual BS distribution, we assume that the location of the BS follows a point process, where the distribution of Voronoi cell area  $V$  still follows (1), but  $c$  becomes a variable controlling the variance of  $V$ . It provides additional adjustability to the BS modeling without adding extra complexity to network performance estimations based on the parameters  $\lambda$  and  $c$ . In this paper,  $V$  [ $\text{km}^2$ ] represents the BS coverage area of its Thiessen polygons [23] when Voronoi Tessellations is used, as shown in Fig. 1.

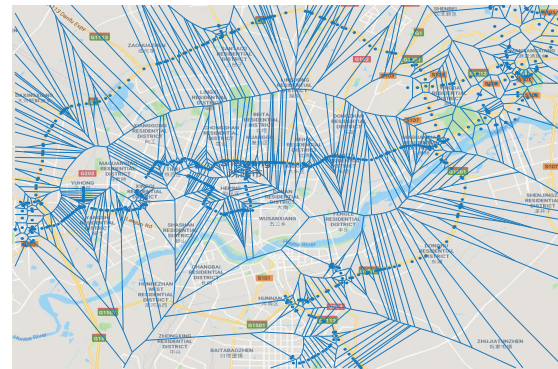
Based on an open-access database containing coordinates and completion time of LTE BSs in an urban region of China [24], we consider the Thiessen polygon area of each BS generated by Voronoi Tessellation as its ideal coverage area. We download an LTE BS database in SQLite file. The data includes LTE BS data of construction date and latitude-longitude coordinates and can be directly extracted by MATLAB. The construction period extracted from the actual data is 32 days, divided into 10 construction stages according to the practical constructed date of these BSs. We calculate statistics of the actual LTE BS coverage areas and their distribution at different construction stages.

Fig. 2 maps BS coverage at both middle and late construction stages. At the unfinished stage of the construction process, operators give priority to cover the populated regions as they are not able to cover all areas in an urgent schedule. As a small number of BSs are expected to cover a large region and to serve massive users, both the expectation and logarithmic variance of the coverage area are large. By contrast, when the network construction is finished, to improve the service probability in all regions, more BSs are deployed. In that case, both the expectation and logarithmic variance of the BS coverage area become smaller when the distribution tends to be uniform.

Correspondingly, Fig. 3 shows that the PDF of coverage areas of real LTE BSs matches that of Voronoi cell area distribution in the modeled point process well. Note that the data of LTE BSs over a city as the empirical data is used



(a) 11th, November, 2016 (the 13rd day)



(b) 31st, November, 2016 (the 32nd day)

**FIGURE 2.** LTE BS maps. Latitude =  $[41.6638^\circ, 41.9170^\circ]$ , Longitude =  $[123.2489^\circ, 123.6980^\circ]$ . The size of the investigated area is  $262.14 \text{ km}^2$ .

as an empirical SCON data in this paper. These LTE BSs will be more clustered by the streets than the ultra-dense SC networks distributed in a smaller area, which will worsen the fitting between the actual data and the theoretical distribution. We foresee that the PDF of actual data will fit better with the theoretical PDF if the SCON data of the ultra-dense SC network can be obtained.

Also, Fig. 3 shows the following construction pattern: with the construction processing, the number of deployed LTE BSs increases, while both  $V_{\text{ave}}(t)$  and  $\sigma(t)$  decrease. To quantitatively describe this pattern, we define  $V_{\text{ave}}(t)$  and  $\sigma(t)$  as functions of time  $t$ . By deducing the formula of  $\frac{\partial V_{\text{ave}}(t)}{\partial t}$  and  $\frac{\partial \sigma(t)}{\partial t}$ , we can derive the relationship between the distribution of BSs and time. A mathematical model that fits the trend of  $V_{\text{ave}}(t)$  and  $\sigma(t)$  in actual SCON network data, can be applied to predict the BS layout at different construction stages in the new SCON model with the similar construction conditions, and thus to predict the network performance at these stages. Therefore, mathematically modeling the variation of the time-varying BS coverage area distribution is crucial for operators to effectively predict the construction period required, and thus operators can use this model to construct an SCON ultra-dense SC network.



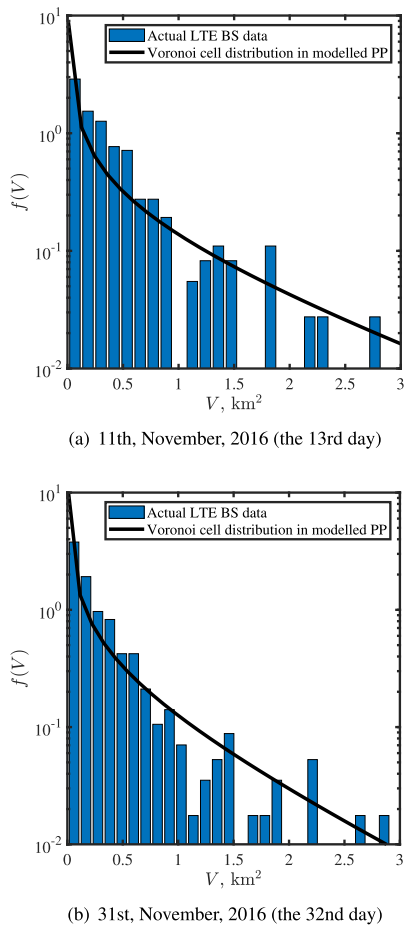


**FIGURE 3.** PDF of coverage areas and Voronoi cell distribution variables in the modeled point process.  $V_{ave} = 0.40$ ,  $\sigma = 1.54$  in (a), and  $V_{ave} = 0.31$ ,  $\sigma = 1.47$  in (b).

### III. FOAM BURSTING PROCESS INSPIRED SCON NETWORK MODEL

The mathematical model of the foam bursting process shows heuristic significance for us to simulate the time-varying distribution of BS coverage areas in an SCON process. Kostoglou *et al.* [17] studied the discipline of the time-varying expectation and logarithmic variance of bubble volume in the bursting process for a large amount of foam in a fixed volume. This foam bursting process is of foam evolving from high density and uniform distribution to low density and non-uniform distribution. The inverse process is enlightening to the coverage area distribution in SCON of ultra-dense SC networks. Besides, similar to the process of foam bursting, the variations of parameters in the BS construction process are discontinuous.

Note that the process of the foam bursting is not precisely the same as the process of SCON, as latter contains more complicated factors. The foam bursting process is caused by the physical mechanisms of the foams, while the BS construction process is caused by the construction planning and the change of hot spots within the construction scope. The foam bursting process is influenced by two main mechanisms. Firstly, the gas in the bubble diffuses through the

liquid membrane from small bubbles (high pressure) to large bubbles (low pressure). The second is that the liquid membrane between adjacent bubbles becomes unstable and eventually breaks, causing the bubbles to merge [25]. These two physical mechanisms advance steadily. In a foam bursting process, these variables, although complex, can be computed by certain formulas [17]. However, the BS construction plan designed according to the reverse process of the foam bursting process is still not the same as the final project result since factors such as weather and holidays affect the construction interval, thus affecting the staged construction of BSs.

Nevertheless, given the gaps in the SCON modeling study, we introduce the inverse foam bursting process as a reference for the BS construction process and ignore the unpredictable factors to make the model more tractable. Generally, investigation on the inverse foam bursting process will still shed light on how SC BSs are deployed due to the similarity of both processes. Therefore, we adopt the inverse foam bursting process model to lay a foundation in this research field.

Based on the foam bursting model [17], we assume the dynamic time-varying functions of the expectation and logarithmic variance for the coverage area of the ultra-dense SC BSs as

$$\frac{\partial V_{ave}(t)}{\partial t} = -kV_{ave}^{q+1}(t) \exp\left(\frac{q^2 - q}{2}\sigma(t)\right), \quad (3)$$

and

$$\frac{\partial \sigma(t)}{\partial t} = -kV_{ave}^q(t) \left[ 2 \exp\left(\frac{q^2 + q - 2}{2}\sigma(t)\right) - \exp\left(\frac{q^2 - q}{2}\sigma(t)\right) \right]. \quad (4)$$

It is noted that, when studying the foam evolution, parameters  $k$  and  $q$  are used to comprehensively describe the changing stability of liquid film between bubbles in the bursting process and thus vary with time. However, parameters  $k$  and  $q$  varying over time will bring more uncertainties in the construction plan, thus lead to a higher computational complexity without increasing the predicting accuracy. In this paper, we decompose  $k$  and  $q$  into two influencing factors for the BS construction process:  $k$  affects construction speed, and  $q$  affects construction uniformity. We assume that  $k$  and  $q$  are static to simplify the analysis, ensuring no additional complexity is involved. With values of  $k$  and  $q$ , which can be extracted from actual BS data, we propose a mathematical model that can fit the distribution change of actual BS coverage area data in Section III, so that the distribution change of the staged constructed BSs in a similar construction scenario can be predicted.

### IV. PARAMETER EXTRACTION ALGORITHM

To simplify (3) and (4), we approximate the differential equations by difference equations as:

$$V_{ave}(t + \Delta t) = V_{ave}(t) - kV_{ave}^{q+1}(t) \times \exp\left(\frac{q^2 - q}{2}\sigma(t)\right) \Delta t, \quad (5)$$

$$\sigma(t + \Delta t) = \sigma(t) - kV_{\text{ave}}^q(t) \times \left[ 2 \exp\left(\frac{q^2+q-2}{2}\sigma(t)\right) - \exp\left(\frac{q^2-q}{2}\sigma(t)\right) \right] \Delta t, \quad (6)$$

where  $\Delta t$  is the sampling interval of the iteration. This mathematical model requires initial values for engineering prediction. The initial values we use are the expectation and logarithmic variance of coverage area obtained at the first sampling time in the actual construction data,  $V_{\text{ave}}(1)$  and  $\sigma(1)$ . According to (2), (5), and (6), temporal variables  $\lambda(t)$  and  $c(t)$  can be computed. In addition,  $\lambda(1)$  and  $c(1)$  derived by  $V_{\text{ave}}(1)$  and  $\sigma(1)$  are also the initial values to simulate the expected theoretical cumulative distribution function (CDF) in the parameter estimation as follows.

According to Kolmogorov theorem [26], the larger the sample size is, the closer the distribution of actual data becomes as compared with the predicted distribution of the fitting model. Thus, on the premise that the actual data samples are reliable enough, the larger the sample size of the initial data is, the more accuracy of the parameter estimation will be. However, the initial values of  $V_{\text{ave}}$  and  $\sigma$  only depend on the initial design of the network by operators in practical engineering applications. In this paper, we mainly study the change of BS deployments in the SCON process. For the initial low-density network deployment designing, many researchers have made relevant works, such as [13], [27]. Operators can refer to these works according to their needs.

To extract values of  $k$  and  $q$  from actual SCON network data, we design an algorithm to estimate these parameter values of  $k$  and  $q$ .

First of all, we design an algorithm to judge whether a set of parameters  $\hat{k}$  and  $\hat{q}$  ensure that the prediction model fits the actual BS construction data at each construction stage. The parameters  $\hat{k}$  and  $\hat{q}$  can be substituted into the difference equations (5) and (6), and we can obtain the theoretical  $V_{\text{ave}}$  and  $\sigma$  at each construction stage, so as to the simulated distribution at each construction stage. The infinite norm between the theoretical CDF of simulated BS distribution,  $\hat{F}_V$ , and the CDF of actual BS distribution at each construction stage,  $F_V$ , is calculated as the Kolmogorov-Smirnov statistic [18] to indicate the accuracy of parameters. The Kolmogorov-Smirnov statistic is denoted by  $\|F_V - \hat{F}_V\|_\infty$ , which fits both  $V_{\text{ave}}$  and  $\sigma$  in the estimation. According to Kolmogorov theorem [26], the square root of the sample size is inversely proportional to the distance between the empirical CDF and the CDF of the estimated model, so the square root of the sample size is used as the weight of the Kolmogorov-Smirnov statistic of each construction stage for estimation, denoted as  $D$ . The model with the smallest Kolmogorov-Smirnov statistic between simulated distribution and actual distribution in all construction stages is considered to have the best parameters  $\hat{k}$  and  $\hat{q}$ , which means the average of  $D$  at all construction stages, denoted as  $D_{\text{mean}}$ .

---

**Algorithm 1**  $D_{\text{mean}}$  Calculating Function

---

**Require:**

- Sampling time  $N_t$ ;
- A set including all BS coverage areas  $d_V$  and their CDF  $F_V(N_t)$  at each sampling time;
- $V_{\text{ave}}(N_t)$  and  $\sigma(N_t)$  at each sampling time;
- The values of parameters  $k$  and  $q$ , denoted as  $\hat{k}$  and  $\hat{q}$ .

**Ensure:**

- The value of  $D_{\text{mean}}$  that is derived from  $\hat{k}$  and  $\hat{q}$ .

```

1:  $k \leftarrow \hat{k}$ ;
2:  $q \leftarrow \hat{q}$ ;
3:  $\hat{V}_{\text{ave}} \leftarrow V_{\text{ave}}(1)$ ;
4:  $\hat{\sigma} \leftarrow \sigma(1)$ ;
5: for  $n = 1 : \text{length}(N_t)$  do
6:    $d_V$  at  $N_t(n)$ ;
7:   if  $n > 1$  then
8:      $t \leftarrow N_t(n) - N_t(n-1)$ ;
9:     for  $m = 1 : N_t(n)$  do
10:       $\hat{V}'_{\text{ave}} \leftarrow \max\left(\hat{V}_{\text{ave}} - k\hat{V}_{\text{ave}}^{q+1} \exp\left(\frac{q^2-q}{2}\hat{\sigma}\right), 0\right)$ 
11:       $\hat{\sigma}' \leftarrow \max\left(\hat{\sigma} - k\hat{V}_{\text{ave}}^q \left[2 \exp\left(\frac{q^2+q-2}{2}\hat{\sigma}\right) - \exp\left(\frac{q^2-q}{2}\hat{\sigma}\right)\right], 0\right)$ 
12:       $\hat{V}_{\text{ave}} \leftarrow \hat{V}'_{\text{ave}}$ 
13:       $\hat{\sigma} \leftarrow \hat{\sigma}'$ 
14:    end for
15:  end if
16:   $\hat{\lambda} \leftarrow \frac{1}{\hat{V}_{\text{ave}}}$ 
17:   $\hat{c} \leftarrow \frac{1}{\exp(\hat{\sigma})-1}$ 
18:   $\hat{F}_V(n) \leftarrow \frac{\Gamma(\hat{c})-\Gamma(\hat{c}, d_V)\hat{\lambda}\hat{c}}{\Gamma(\hat{c})}$ 
19:   $D(n) \leftarrow \sqrt{\text{length}(d_V)} \cdot \|F_V - \hat{F}_V\|_\infty$ 
20:   $D_{\text{mean}} \leftarrow \text{mean}(D)$ 
21: end for
22: return  $D_{\text{mean}}$ .

```

---

should be the smallest. The detailed steps of the function that computing  $D_{\text{mean}}$  from parameters  $\hat{k}$  and  $\hat{q}$  are presented in Algorithm 1. When comparing the actual BS construction data with the fitted model, the CDFs of the fitted model and the corresponding actual CDFs at 10 construction stages are compared respectively.

The best estimation results of  $k$  and  $q$  from the potential range of  $\hat{k}$  and  $\hat{q}$  are  $k$  and  $q$  that can minimize the value of  $D_{\text{mean}}$ . To constrain the minimization of the  $D_{\text{mean}}$ , denoted as  $D_{\text{best}}$ , the interior-point approach [28] is applied to quickly compute the optimal solution in the estimation interval of parameters  $\hat{k}$  and  $\hat{q}$ , as shown in Algorithm 2.

## V. NUMERICAL RESULTS

### A. HISTORICAL DATA-BASED VALIDATION

To verify the parameter estimation algorithm, we list the  $D_{\text{mean}}$  results with different values of parameters  $k$  and  $q$ , as shown in Fig. 4. The minimum  $D_{\text{mean}} = 1.85$  is

**Algorithm 2** Minimization Constraint Algorithm**Require:**

- $D_{\text{mean}}$  Calculating Function (Algorithm 1), denoted as Fun;
- The potential range of  $\hat{k}$  and  $\hat{q}$ .
- The initial values  $k_0$ , and  $q_0$ , ensuring that  $k_0 \in \hat{k}$  and  $q_0 \in \hat{q}$ .

**Ensure:**

- The minimum  $D_{\text{mean}}$  that can be derived in the potential range, denoted as  $D_{\text{best}}$ ;
- The  $k$  and  $q$  that derive  $D_{\text{best}}$ .

```

1:  $\mathbf{lb} \leftarrow [\min(\hat{k}), \min(\hat{q})]$ ;
2:  $\mathbf{ub} \leftarrow [\max(\hat{k}), \max(\hat{q})]$ ;
3:  $\mathbf{x}_0 \leftarrow [k_0, q_0]$ ;
4:  $[\mathbf{x}, D_{\text{best}}] \leftarrow \text{fmincon}(\text{Fun}, \mathbf{x}_0, [], [], [], [], \mathbf{lb}, \mathbf{ub})$ ;
5:  $k \leftarrow \mathbf{x}(1)$ ;
6:  $q \leftarrow \mathbf{x}(2)$ ;
7: return  $k, q, D_{\text{best}}$ 

```

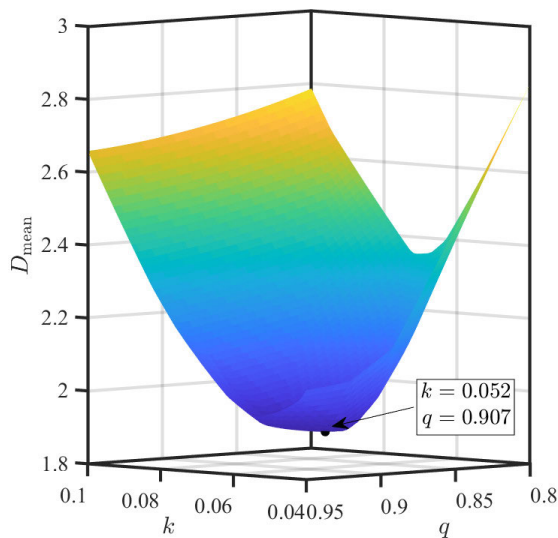


**FIGURE 4.** The average Kolmogorov-Smirnov statistic  $D_{\text{mean}}$  that calculated by Algorithm 1. The lowest point shows the best result ( $q = 0.91$ ,  $k = 0.05$ ) that minimizing the  $D_{\text{mean}} = 1.85$ . This minimum  $D_{\text{mean}}$  can be quickly found when Algorithm 2 is applied without enumerating all  $D_{\text{mean}}$ .

found when  $k$  is 0.05 and  $q$  is 0.91, illustrating that the Algorithm 2 can effectively find the optimal solution to minimize  $D_{\text{mean}}$ .

By substituting the values of the best  $\hat{k}$  and  $\hat{q}$  into (5), (6), we have:

$$V_{\text{ave}}(t + \Delta t) = V_{\text{ave}}(t) - 0.05 V_{\text{ave}}^{1.91}(t) \times \exp(-0.04\sigma(t))\Delta t, \quad (7)$$

$$\sigma(t + \Delta t) = \sigma(t) - 0.05 V_{\text{ave}}^{0.91}(t) \times [2 \exp(-0.13\sigma(t)) - \exp(-0.04\sigma(t))] \Delta t. \quad (8)$$

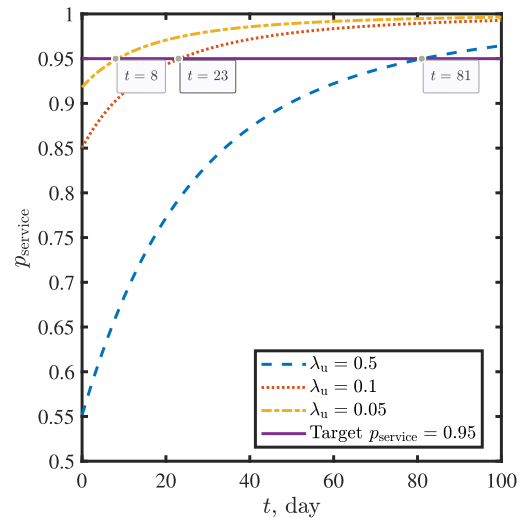


**FIGURE 5.** Service probability  $p_{\text{service}}$  prediction of the under-construction interference-limited network for different MU density  $\lambda_u$ , where the path loss exponent is  $\alpha = 4$ , and the target SINR is  $\hat{\gamma} = 0$  dB. Calculation of  $p_{\text{service}}$  is referred to Equation (5) in [22].

Equations (7) and (8) can be used to estimate the time-varying expectation and logarithmic variance of BS coverage areas in similar construction scenarios. Then, we predict the trends of  $V_{\text{ave}}$  and  $\sigma$  from the initial  $V_{\text{ave}}$  as  $V_{\text{ave}}(1)$  and initial  $\sigma$  as  $\sigma(1)$  by iterating over (7) and (8) with  $\Delta t$  as 1 day.

**B. CASE STUDY**

Combining (2), (7) and (8), the time-varying distribution of BS coverage areas can be derived. The actual BS construction data is thus converted into an empirical model. By combining this empirical SCON model with the existing solution for calculating the network service probability based on the Voronoi cell area distribution [22], we obtain the service probability of an under-construction interference-limited network for different MU density  $\lambda_u$ , where the path loss exponent  $\alpha = 4$ , and the target signal to interference and noise ratio (SINR)  $\hat{\gamma} = 0$  dB, as shown in Fig. 5. Note that the actual BS data is used to simulate the ultra-dense SC network, so that the densities of mobile users (MUs) are set to be 1 dB to 3 dB lower than the BS density (the BS density  $\lambda = 6.97$  BSs/km<sup>2</sup> at the end of the construction when  $t = 100$  days).

When the operator set the target service probability (95% in Fig. 5), the expected period of a network construction scheme can be deduced through this model to evaluate whether the construction scheme, determined by  $k$  and  $q$ , is acceptable for this new SCON project. For example, if the target MU density of the network is 0.5 UEs/km<sup>2</sup> and the scheduled construction period is 80 days, the operators reject this construction scheme. On the contrary, if the target MU density of the network is 0.05 UEs/km<sup>2</sup>, and the scheduled construction period is 10 days, then this construction scheme can be considered acceptable.

It should be acknowledged that the actual BS density in the ultra-dense SC network will be much higher than the density of the actual BS data used in this paper.

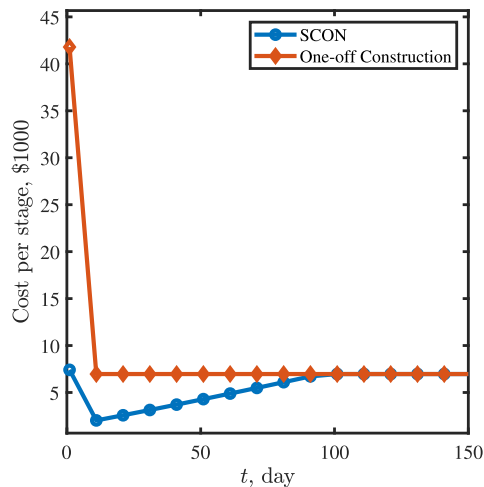


**FIGURE 6.** The total cost of every construction stage estimation for the SCON network and a one-off deployed network with the same construction scale. The CAPEX per cell is set as  $\text{capex} = \$5000$ , and the OPEX per cell is set as  $\text{opex} = \$1000$ . The target coverage range of the network  $S = 1\text{km}^2$ . The actual cost data is referred from [11].

The proposed dynamic model for SCON SC network performance evaluation will evolve once the operators own the SCON data of an ultra-dense SC network. Fed with big SCON data, the proposed model lays a foundation to provide the design basis for the future ultra-dense SC network SCON projects.

### C. COST ESTIMATION

In a network, according to [11], the CAPEX of each cell can be decomposed into the cost of the cell and the cost of the core network working on the cell, while the periodic OPEX per cell includes marketing costs, electricity bill, venue rental, back-haul rental, as well as the hardware and software maintenance costs. The cost estimation model can be simplified when assuming the CAPEX and OPEX of each cell as fixed values, denoted as  $\text{capex}$  and  $\text{opex}$ . Clearly that the CAPEX and OPEX of the under-constructed network at the construction stage  $t$  are related to the constructed BS number  $N(t)$  and the under-constructed BS number  $N(t + \Delta t) - N(t)$  at this construction stage:

$$\text{CAPEX}(t) = \varphi_{\text{capex}} \times (N(t + \Delta t) - N(t)), \quad (9)$$

$$\text{OPEX}(t) = \varphi_{\text{opex}} \times N(t), \quad (10)$$

where  $N(t) = S \times \lambda(t)$ , and  $S$  refers to the target coverage range of the network.

Combining (9), (10) with the actual cost data referred from [11], we estimate the total cost of every construction stage as the sum of  $\text{CAPEX}(t)$  and  $\text{OPEX}(t)$  of the empirical SCON model generated in Section V.B. The construction is assumed to be finished in day 100. The estimation result of cost per stage is shown in Fig. 6, with the costs of a one-off deployed network with the same construction scale plotted as comparisons.

Fig. 6 clearly shows that a one-off deployment strategy results in significant initial investment requirements. In contrast, the SCON strategy would dilute this massive

investment by a more extended construction period, reducing the operators financing difficulty. Moreover, all SCs have been deployed at the beginning of the one-off construction. That makes the OPEX of the one-off deployed network higher than that of the SCON network. The OPEX of the completed SCON network rises to the same as the one-off deployed network.

### VI. CONCLUSION AND FUTURE WORK

In this paper, a mathematical model to describe the time-varying distribution of SC BS coverage areas in an SCON network has been proposed. The model was inspired by the foam bursting process. Moreover, parameters of this time-varying model have been estimated using actual BS data, and an empirical model has been obtained for future SC network deployment using the SCON approach. Combined with the existing network evaluation solutions, this mathematical model can help operators effectively evaluate whether a construction scheme generated by a completed SCON data is acceptable for designing new SCON networks. Since no available SCON data of ultra-dense SC networks exists at this moment, the proposed model is validated by comparing the distribution of BS coverage areas obtained by this mathematical model with actual LTE networks, which were built at a limited number of stages. With the large-scale deployment of ultra-dense SC networks, the increasing amount of reference data will make this model more accurate.

In the future, our model will evolve as the SCON data access increase. Thus, we will continue to study the SCON process mechanism in combination with economics, psychology, geography, and other interdisciplinary subjects. Moreover, since our work and the reviewed dynamic networks modeling in the field of self-organizing networks and BS on/off switch handling are focusing on the network at different construction states, we will combine our work with existing dynamic network models to optimize the network performance at different construction stages.

### REFERENCES

- [1] D. Lopez-Perez, I. Guvenc, G. de la Roche, M. Kountouris, T. Quek, and J. Zhang, "Enhanced intercell interference coordination challenges in heterogeneous networks," *IEEE Wireless Commun.*, vol. 18, no. 3, pp. 22–30, Jun. 2011.
- [2] M. A. Adedoyin and O. E. Falowo, "Combination of ultra-dense networks and other 5G enabling technologies: A survey," *IEEE Access*, vol. 8, pp. 22893–22932, 2020.
- [3] X. Ge, S. Tu, G. Mao, and C. X. Wang, "5G ultra-dense cellular networks," *IEEE Trans. Wireless Commun.*, vol. 23, no. 1, pp. 72–79, Feb. 2016.
- [4] M. M. A. Hossain, K. Koufos, and R. Jantti, "Energy efficient deployment of HetNets: Impact of power amplifier and delay," in *Proc. IEEE Wireless Commun. Netw. Conf. (WCNC)*, Apr. 2013, pp. 778–782.
- [5] F. Richter, A. J. Fehske, and G. P. Fettweis, "Energy efficiency aspects of base station deployment strategies for cellular networks," in *Proc. IEEE 70th Veh. Technol. Conf. Fall*, Sep. 2009, pp. 1–5.
- [6] Y. Chen, M. Ding, and D. Lopez-Perez, "Performance of ultra-dense networks with a generalized multipath fading," *IEEE Wireless Commun. Lett.*, vol. 8, no. 5, pp. 1419–1422, Oct. 2019.
- [7] F. Mohammadnia, M. Fiore, and M. A. Marsan, "Adaptive densification of mobile networks: Exploring correlations in vehicular and telecom traffic," in *Proc. 17th Annu. Medit. Ad Hoc Netw. Workshop (Med-Hoc-Net)*, Jun. 2018, pp. 1–8.



- [8] M. Gao, J. Li, D. N. K. Jayakody, H. Chen, Y. Li, and J. Shi, "A super base station architecture for future ultra-dense cellular networks: Toward low latency and high energy efficiency," *IEEE Commun. Mag.*, vol. 56, no. 6, pp. 35–41, Jun. 2018.
- [9] C. Chen, S. Yang, J. Zhang, X. Chu, and J. Zhang, "Tractable performance analysis of small-cell networks with a novel bounded path loss model," *Electron. Lett.*, vol. 56, no. 2, pp. 105–107, Jan. 2020.
- [10] G. Zhao, S. Chen, L. Zhao, and L. Hanzo, "Energy-spectral-efficiency analysis and optimization of heterogeneous cellular networks: A large-scale user-behavior perspective," *IEEE Trans. Veh. Technol.*, vol. 67, no. 5, pp. 4098–4112, May 2018.
- [11] W. Guo and T. O'Farrell, "Capacity-energy-cost tradeoff in small cell networks," in *Proc. IEEE 75th Veh. Technol. Conf. (VTC Spring)*, May 2012, pp. 1–5.
- [12] J. J. Phillips, *Return on Investment in Training and Performance Improvement Programs*. Evanston, IL, USA: Routledge, 2012.
- [13] H. Klessig, D. Ohmann, A. I. Reppas, H. Hatzikirou, M. Abedi, M. Simsek, and G. P. Fettweis, "From immune cells to self-organizing ultra-dense small cell networks," *IEEE J. Sel. Areas Commun.*, vol. 34, no. 4, pp. 800–811, Apr. 2016.
- [14] P. Semov, H. Al-Shatri, K. Tonchev, V. Poulkov, and A. Klein, "Implementation of machine learning for autonomic capabilities in self-organizing heterogeneous networks," *Wireless Pers. Commun.*, vol. 92, no. 1, pp. 149–168, Jan. 2017.
- [15] B. Shubyn, N. Lutsiv, O. Syrotynskyi, and R. Kolodii, "Deep learning based adaptive handover optimization for ultra-dense 5G mobile networks," in *Proc. IEEE 15th Int. Conf. Adv. Trends Radioelectronics, Telecommun. Comput. Eng. (TCSET)*, Feb. 2020, pp. 869–872.
- [16] L. N. de Castro, "Fundamentals of natural computing: An overview," *Phys. Life Rev.*, vol. 4, no. 1, pp. 1–36, Mar. 2007.
- [17] M. Kostoglou, J. Lioumbas, and T. Karapantsios, "A population balance treatment of bubble size evolution in free draining foams," *Colloids Surf. A, Physicochem. Eng. Aspects*, vol. 473, pp. 75–84, May 2015.
- [18] F. J. Massey, "The Kolmogorov-Smirnov test for goodness of fit," *J. Amer. Stat. Assoc.*, vol. 46, no. 253, pp. 68–78, Mar. 1951.
- [19] J. G. Andrews, F. Baccelli, and R. K. Ganti, "A tractable approach to coverage and rate in cellular networks," *IEEE Trans. Commun.*, vol. 59, no. 11, pp. 3122–3134, Nov. 2011.
- [20] M. Di Renzo, "Stochastic geometry modeling and analysis of multi-tier millimeter wave cellular networks," *IEEE Trans. Wireless Commun.*, vol. 14, no. 9, pp. 5038–5057, Sep. 2015.
- [21] J.-S. Ferenc and Z. Nédá, "On the size distribution of Poisson Voronoi cells," *Phys. A, Stat. Mech. Appl.*, vol. 385, no. 2, pp. 518–526, Nov. 2007.
- [22] S. M. Yu and S.-L. Kim, "Downlink capacity and base station density in cellular networks," in *Proc. 11th WiOpt*, 2013, pp. 119–124.
- [23] P. A. Burroughs, R. A. McDonnell, and C. D. Lloyd, *Principles of Geographical Information Systems*. Oxford university press, 2015.
- [24] Radiocells. *Cell and WiFi Data*. Accessed: Jul. 18, 2019. [Online]. Available: <https://www.radiocells.org/downloads>
- [25] D. L. Weaire and S. Hutzler, *The Physics of Foams*. London, U.K.: Oxford Univ. Press, 2001.
- [26] A. Kolmogorov-Smirnov, A. Kolmogorov, and M. Kolmogorov, "Sulla determinazione empirica di una legge di distribuzione," *Inst. Ital. Attuari, Giorn.*, vol. 4, pp. 83–91, 1933.
- [27] Y. Wu and Z. Niu, "Energy efficient base station deployment in green cellular networks with traffic variations," in *Proc. 1st IEEE Int. Conf. Commun. China (ICCC)*, Aug. 2012, pp. 399–404.
- [28] R. H. Byrd, J. C. Gilbert, and J. Nocedal, "A trust region method based on interior point techniques for nonlinear programming," *Math. Program.*, vol. 89, no. 1, pp. 149–185, Nov. 2000.



research interests include stochastic geometry, queuing theory, interference management, heterogeneous networks, Fog-RAN, and NR-U networks.

**HAONAN HU** (Member, IEEE) received the B.S. degree from the Beijing University of Posts and Telecommunications, China, in 2010, the M.S. degree from the Chongqing University of Posts and Telecommunications, China, in 2013, and the Ph.D. degree from the Department of Electronic and Electrical Engineering, The University of Sheffield, Sheffield, U.K., in 2019. He is currently an Associate Professor with the Chongqing University of Posts and Telecommunications. His



Engineering, Chalmers University of Technology, Gothenburg, Sweden, from 2017 to 2018. He is currently a Marie Curie Research Fellow with the Department of Electronic and Electrical Engineering, The University of Sheffield, Sheffield, U.K. His current research interests include, but are not limited to, wireless channel modeling, modulation systems, relay systems, wireless ranging systems, vehicular communications, ultra-dense small cell networks, and smart environment modeling.

**JILIANG ZHANG** (Senior Member, IEEE) received the B.E., M.E., and Ph.D. degrees from the Harbin Institute of Technology, Harbin, China, in 2007, 2009, and 2014, respectively. He was a Postdoctoral Fellow with the Shenzhen Graduate School, Harbin Institute of Technology, from 2014 to 2016, an Associate Professor with the School of Information Science and Engineering, Lanzhou University, from 2017 to 2019, and a Researcher with the Department of Electrical



Ranplan Professional and Collaboration-Hub, which are being used by the world's largest mobile operators and network vendors across the globe. Along with his students and colleagues, he has pioneered research in small cell and heterogeneous network (HetNet) and published some of the landmark papers and books on these topics, widely used by both academia and industry. Prior to his current appointments, he studied and worked at Imperial College London, Oxford University, the University of Bedfordshire, and the East China University of Science and Technology, reaching the rank of a Lecturer, Reader, and Professor in 2002, 2005, and 2006, respectively. He has published some of the earliest articles on using social media network data for proactive network optimization. Since 2010, he and his team have been developing ground-breaking work in modeling and designing smart built environments considering both wireless and energy efficiency. His Google Scholar citations are in excess of 7000 with an H-index of 37.

**JIE ZHANG** (Senior Member, IEEE) has been the Chair of Wireless Systems with the Department of Electronic and Electrical Engineering, The University of Sheffield, since January 2011. He is also the Founder, Board Chairman, and Chief Scientific Officer (CSO) at Ranplan Wireless, a public company listed on Nasdaq OMX. Ranplan Wireless produces a suite of world leading indoor and the only joint indoor-outdoor 5G/4G/WiFi network planning and optimization tools suites, including



**YIXIN HUANG** received the B.Eng. degree in measurement and control technology and instrumentations from Xi'an Jiaotong University, Xi'an, China, in 2015. She is currently pursuing the Ph.D. degree with the Department of Electronic and Electrical Engineering, The University of Sheffield, Sheffield, U.K. Her research interests include dynamic network modeling, UAV networks, and machine learning.